Published in final edited form as:
Ann Neurol. 2011 September ; 70(3): 362–373. doi:10.1002/ana.22449.

Japanese macaque encephalomyelitis: a spontaneous multiple sclerosis-like disease in a nonhuman primate

Michael K. Axthelm, D.V.M., Ph.D.[1,2], **Dennis N. Bourdette, M.D.**[3], **Gail H. Marracci, Ph.D.**[3], **Weiping Su, Ph.D.**[4], **Elizabeth T. Mullaney, B.S.**[2], **Minsha Manoharan, M.S.**[2], **Steven G. Kohama, Ph.D.**[4], **Jim Pollaro, M.S.**[5], **Ellen Witkowski, B.A.**[4], **Paul Wang, M.D.**[5], **William D. Rooney, Ph.D.**[5], **Lawrence S. Sherman, Ph.D.**[4], and **Scott W. Wong, Ph.D.**[1,2,6]

[1]Division of Pathobiology and Immunology, Oregon National Primate Research Center, Beaverton, OR 97006

[2]Vaccine and Gene Therapy Institute, Oregon Health & Science University, Beaverton, OR 97006

[3]Neurology and Research Service, Department of Veterans Affairs Medical Center and Department of Neurology, Oregon Health & Science University, Portland, OR 97239

[4]Division of Neuroscience, Oregon National Primate Research Center, Beaverton, OR 97006

[5]Advanced Imaging Research Center, Oregon Health & Science University, Portland, OR 97239

[6]Department of Molecular Microbiology and Immunology, Oregon Health & Science University, Portland, OR 97239

Abstract

Objective—To describe Japanese macaque encephalomyelitis (JME), a spontaneous inflammatory demyelinating disease occurring in the Oregon National Primate Research Center's (ONPRC) colony of Japanese macaques (JM, *Macaca fuscata*).

Methods—JM with neurologic impairment were removed from the colony, evaluated and treated with supportive care. Animals were humanely euthanized and their central nervous system (CNS) examined.

Results—ONPRC's JM colony was established in 1965 and no cases of JME occurred until 1986. Since 1986, 56 JM spontaneously developed a disease characterized clinically by paresis of one or more limbs, ataxia or ocular motor paresis. Most animals were humanely euthanized during their initial episode. Three recovered, later relapsed and were then euthanized. There was no gender predilection and the median age for disease was 4 years. Magnetic resonance imaging of eight cases of JME revealed multiple gadolinium enhancing T1-weighted hyperintensities in the white matter of the cerebral hemispheres, brainstem, cerebellum and cervical spinal cord. The CNS of monkeys with JME contained multifocal plaque-like demyelinated lesions of varying ages, including acute and chronic, active demyelinating lesions with macrophages and lymphocytic periventricular infiltrates, and chronic, inactive demyelinated lesions. A previously undescribed gamma-herpesvirus was cultured from acute JME white matter lesions. Cases of JME continue to affect 1–3% of the ONPRC colony per year.

Interpretation—JME is a unique spontaneous disease in a nonhuman primate that has similarities with multiple sclerosis (MS) and is associated with a novel simian herpesvirus. Elucidating the pathogenesis of JME may shed new light on MS and other human demyelinating diseases.

Corresponding author, Scott W. Wong, Ph.D., Vaccine and Gene Therapy Institute, 505 NW 185th Avenue, Beaverton, OR 97006, Phone: 503-690-5285, wongs@ohsu.edu.

INTRODUCTION

Multiple sclerosis (MS) is a chronic inflammatory disease that affects the central nervous system (CNS). The disease typically follows a relapsing-remitting course and is associated with a variety of neurological deficits, such as paralysis, imbalance, ataxia, blindness and ocular motor paresis (reviewed in [1]). Classically, the pathology of MS consists of discrete, multifocal areas of demyelination, associated with variable axonal loss in the white matter of the brain, spinal cord and optic nerves. More recently, lesions within the grey matter have been described. Lesions with active demyelination are associated with infiltrating lymphocytes and lipid-laden phagocytic macrophages. Although the cause of MS remains uncertain, there is considerable evidence indicating that multiple genetic loci and incompletely understood environmental exposures influence the risk of developing MS (reviewed in [2]). One still unproven hypothesis is that a viral infection occurring in genetically susceptible individuals induces the disease.

The most widely studied model of MS is experimental autoimmune encephalomyelitis (EAE) (reviewed in [3]). This paralytic illness can be induced in a variety of mammalian species by immunization with whole myelin or specific myelin proteins, most notably myelin basic protein (MBP), myelin oligodendrocyte glycoprotein and proteolipid protein, or peptides from these proteins[4–6]. Depending on the species used and method of disease induction, EAE can follow a chronic relapsing course and be associated with multifocal areas of demyelination and thus mimic MS pathologically and clinically[7]. There are also mouse models of virally induced demyelinating diseases, most notably Theiler's murine encephalomyelitis virus (TMEV)[8–10]. TMEV-induced demyelinating disease (TMEV-IDD) is induced by injecting neurotropic strains of the virus into genetically susceptible mice[11]. Depending upon the strain of TMEV, infection can result in either acute encephalitis or a chronic immune-mediated multifocal demyelinating disease. While EAE can be induced in rhesus and common marmoset monkeys, a virally induced model of MS has not been described in nonhuman primates (NHP). Availability of a demyelinating disease associated with a virus in an NHP might prove relevant to understanding the pathogenesis of MS.

Here, we report the spontaneous occurrence of an inflammatory demyelinating disease in a colony of Japanese macaques (JM, *Macaca fuscata*) at the Oregon National Primate Research Center (ONPRC). The disease, Japanese macaque encephalomyelitis (JME), has clinical and pathologic similarities with MS. Moreover, we report the isolation of a previously undescribed simian herpesvirus isolated from acute JME lesions. This is the first description of a spontaneously occurring MS-like disease in a NHP and has the potential to offer new insights into the pathogenesis of MS.

MATERIAL AND METHODS

Animals

All animal procedures were approved by the ONPRC Institutional Animal Care and Use Committee. The ONPRC is an Association for Assessment and Accreditation of Laboratory Animal Care International accredited research facility and conforms to National Institutes of Health guidelines on the ethical use of animals in research. The JM colony is maintained in a two-acre corral and members of the colony are observed daily for the presence of sick or injured animals. Per institutional protocol, members of the colony developing neurologic dysfunction were removed from the corral, placed in cages, evaluated and provided supportive care. Most animals developing JME were humanely euthanized per ONPRC protocol. Three animals recovered from their initial episode, were returned to the corral, but later relapsed and then were humanely euthanized.

Clinical sample analysis

Cerebrospinal fluid (CSF) was acquired from sedated animals and analyzed for total protein, cell count and cell type determination. Complete blood count and routine serum chemistries were obtained.

Histopathological examination

Complete necropsies were performed on all animals. CNS tissues were collected from most animals and either placed in neutral-buffered formalin or neutral-buffered 4% paraformaldehyde for paraffin embedding or media for isolation of a potential infectious agent. Sections from the CNS were cut at 5 μm, deparaffinized and stained with hematoxylin and eosin, Luxol fast blue-PAS-hematoxylin stain or Bielschowsky's silver impregnation to image axons, or blocked with 5% normal goat serum and 5% bovine serum albumin for immunostaining with primary antibodies specific for MBP (rabbit anti-MBP, Zymed; 1:100), neurofilament (NF) light chain (mouse anti-NF, Chemicon; 1:500), oligodendrocytes lineage transcription factor 2 (olig2) (rabbit anti-olig2, Chemicon; 1:500), T cells (rabbit anti-CD3, Dako; 1:200) or macrophages (mouse anti-CD68, Dako; 1:80). Secondary antibodies used were: goat-anti-rabbit IgG conjugated to Alexa 488 (Molecular Probes; 1:500), goat-anti-mouse IgG conjugated to Alexa 546 (Molecular Probes; 1:500), biotinylated goat-anti-rabbit IgG and biotinylated goat-anti-mouse IgG. Streptavidin-Alexa 488 and Streptavidin-Alexa 594 were utilized to visualize CD3+ T cells and CD68+ macrophages, respectively. The sections were then counterstained with 3,3'-diaminobenzidine (DAP)I (1:5000) and analyzed by light or fluorescent microscopy performed on a Zeiss microscope equipped with an Axiocam digital camera.

For quantitation of olig2-immunolabeled cells, three adjacent sections were analyzed at 40× following double labeling with anti-MBP and anti-olig2 antibodies. Three regions of interest (ROI) were identified using MBP labeling: the lesion, where MBP immunoreactivity was mostly absent; the border, where there was a mixture of intact myelin and damaged myelin; adjacent unaffected white matter. The number of olig2+ cells in three random microscopic fields within each ROI in each adjacent section was then counted and averaged. The mean differences between ROIs were assessed using Student's t test.

Magnetic resonance imaging

A 4 year 240 day old female JM exhibiting signs of JME was transported to Oregon Health & Science University Hospital and positioned in a General Electric 1.5 Tesa (T) Signa MRI instrument and T2 weighted and pre- and post-gadolinium T1 weighted images were obtained from the brain and cervical cord. All other MRIs were performed on a 3 Tesa Siemens Trio whole-body MRI instrument using a quadrature transmit/receive extremity radiofrequency coil. Sixty sagittally oriented 2D turbo spin echo acquisitions with proton density (TE17/TR9000/ETL9/NEX1) contrast were collected with a 1 mm slice thickness and 256×256 matrix over a 160mm^2 field-of-view (FOV). Multislice 2D turbo spin echo MRI acquisitions with proton density (TE13/TR9000/ETL9/NEX2) and T_2-weighted (TE92/TR9000ETL9/NEX2) contrast were collected in an axial orientation angulated parallel to the imaginary line connecting the anterior and posterior commissures; 66 1 mm slices were collected using a 320×240 matrix over a 160mm×120mm field-of-view (FOV). Transaxial 3D T_1-weighted Magnetization Prepared Rapid Acquisition Gradient Echo (MPRAGE); TE3.5/TR2500/TI900/FA8) data sets were acquired before and 30 minutes after gadoteridol administration with a 192×144×96 matrix over a 130mm×98mm×76mm field-of-view (FOV). Gadoteridol was administered in situ at a dose of 0.2 mmol/kg using an infusion pump.

Isolation of a herpesvirus from an acute lesion

A spinal lesion from a JM (#17792) with JME was obtained at necropsy, homogenized and placed over primary rhesus macaque fibroblasts for isolation and analysis of a potential infectious agent as described[12]. Preliminary molecular characterization to identify the herpesvirus was conducted as described[12]. Using the same technique, attempts were made to isolate viruses from other acute JME lesions and normal white matter from JM with and without JME.

RESULTS

Japanese macaque encephalomyelitis

The ONPRC has housed an outbred colony of JM since 1965. No cases of unexplained neurologic disease were observed in the colony prior to 1986. Since 1986, 56 JM spontaneously developed JME (Figure 1). Currently, 1–3% of the colony develops JME each year and the disease affects males and females equally. Except for the burst of cases in August 1987, there is no apparent seasonal predilection and cases have occurred every year since 1986 except in 1993 and 2004. Table 1 provides details of the clinical features of the disease on the 56 cases. The median age of affected animals was 4 years 109 days (range, 97 days-26 years 50 days). The majority of the animals had paresis or paralysis of one or more limbs and ataxia. Ocular paresis occurred in 10 cases. Seven animals exhibited other clinical manifestations, including abnormal species-specific behaviors and head tilt accompanied with body tremors. Typically, the onset of clinical disease was acute and progressed rapidly with the median time between presentation of disease to humane euthanasia being 6 days (range, 0 days-121 days). In most cases, euthanasia was required because neurologic impairment made it impossible to return the monkeys safely to the colony. Three animals (#12068, 21255 and 16749) recovered from their initial episode and were returned to the corral, but were later euthanized when their JME recurred 101 days-8 years later.

CSF was collected on 40 affected animals. The mean CSF white blood cell (WBC) count was 185 cells/mm^3 with a range from 0 to 2,710. WBC differential was obtained in 13 cases and in all but one the cells consisted of both lymphocytes and neutrophils. The mean total protein was 52 mg/dL (range, 0–195 mg/dL). Glucose values were normal and attempts to isolate bacteria from CSF were negative. Hematological and biochemical examinations of blood revealed no consistent abnormalities. CSF was not examined for oligoclonal bands or IgG index.

MRI abnormalities

MRI scans were performed on eight animals with JME and MRI scans from three cases are shown in Figure 2. A brain and cervical MRI scan was performed on JM #19384 11 days after presentation with clinical signs of JME (Figure 2A–C). Post-gadolinium T_1-weighted images revealed multiple areas of focal contrast enhancement in the white matter of the cerebral hemispheres, cerebellum, brainstem and cervical cord. JM #26174 underwent MRI 4 days after presentation with acute JME signs (Figure 2D–I). The T_2-weighted axial images in D-F showed hyperintense areas in the upper cervical cord, cerebellum and cerebrum. The axial images of G-I show intense focal contrast enhancement in the upper cervical cord, cerebellum and genu of the corpus callosum. JM #13221 underwent MRI 3 days after presentation with acute JME symptoms (Figure 2J–L). T_2-weighted axial images revealed a large hyperintense area in the left cerebral peduncle (Figure 2J). The same area had a hypointense appearance in the T_1-weighted MPRAGE image (Figure 2K). Punctate gadolinium enhancement was apparent in this same peduncle region in the post-contrast T_1-weighted image (Figure 2L). The MRI abnormalities displayed here are similar to those of

the other five cases of JME that underwent MRI, consistent with active neuroinflammation and similar to the MRI findings of acute lesions in MS.

Neuropathology

Complete necropsies were performed on 54/56 cases of JME. No monkeys had evidence of a systemic illness or acute disease outside of the CNS. In all cases, neuropathologic examination of the brain and cervical spinal cord revealed a multifocal demyelinating encephalomyelitis. In most cases, multiple, dull, yellow-white to gray-tan, well-delineated plaques that ranged from 0.2 to 1.0 cm in greatest dimension were apparent on gross inspection of post-fixed coronal brain and spinal cord slices. Gross lesions were most frequent in the cerebellar white matter, brachium pontis, pyramids and the white matter of the cervical spinal cord. A typical distribution of plaque-like lesions in the cerebellum and spinal cord was found in animal #19384 that underwent MRI (Figure 3A). Histologically, a majority of lesions seen in all JME cases had morphologic features consistent with the chronic active plaques described in MS[13–17]. Plaques were typically centered on venules or small veins. The chronic active plaques (Figure 3B) were dominated centrally by macrophages engorged with myelin debris intermingled with astrocytes. Infiltrating macrophages and lymphocytes dominated in peripheral portions of plaques with focal concentrations of lymphocytes forming perivascular cuffs. Areas of necrosis and microcystic spaces were occasionally observed in the central portion of chronic-active lesions. Variations in lesion age were observed in some animals. Early lesions were infrequent and characterized by perivenous lymphocytic cuffs that frequently tracked perforating venules from piaarachnoid surfaces into adjacent white matter. The adjacent myelin was vesiculated and sparsely infiltrated with lymphocytes and macrophages. Rarely, small focal hemorrhages were encountered in the edematous myelin. Chronic inactive plaques composed principally of astrocytes and foamy macrophages were seen in many of the animals (Figure 3C). Lymphocytes were largely absent in these lesions and silver staining revealed decreased numbers of axons with evidence of acute axotomies (Figure 3D and E). Regardless of apparent age, lesions were exclusively located in white matter in all animals. Apart from rare, small, perivascular collections of lymphocytes, lesions were not seen in grey matter or the meninges. Transmission electron microscopy (EM) was performed on a limited number of lesions and these disclosed degenerating axons, demyelinated axons and occasional thinly myelinated axons, suggesting remyelination (data not shown).

Immunostaining was performed on two lesions localized by MRI in animal #13221. The first lesion was analyzed by immunostaining for alterations in MBP, NF, and olig2 immunoreactivity, and a second for infiltration of macrophages and T cells. MBP and NF labeling demonstrated areas with axon and myelin debris (defined as the demyelinated lesion) adjacent to border areas showing a mixture of intact and damaged fibers, which was, in turn, adjacent to unaffected white matter (Figure 4A and B). Staining for the presence of CD68 in a lesion located in the cerebellum revealed numerous CD68+ macrophages and perivascular CD3+ T cells (Figure 4C). Oligodendrocytes were quantified by enumerating olig2-labeled cells within the lesion shown in Figure A and B. There was nearly complete absence of olig2 immunoreactivity within the lesion and a dramatic reduction in olig2+ cells at the lesion border compared to adjacent unaffected white matter (Figure 4D and E). The lesions of JME thus are multifocal, contain T cell and macrophage infiltrates and reveal demyelination, loss of oligodendrocytes, limited remyelination, and axonal degeneration.

Isolation of novel gamma-2 herpesvirus from encephalomyelitis lesions

As viral infection has been associated with inflammatory demyelination in mice, we investigated whether a virus might be present in acute lesions of animals with JME. Explant cultures of lesioned spinal cord tissue versus normal neuronal tissue from JM #17792

layered over primary rhesus fibroblasts yielded an infectious agent that was identified by transmission EM as a herpesvirus (data not shown). The virus isolate was subsequently passaged and viral DNA purified from cell-free virions for degenerate PCR amplification over a highly conserved region of the viral DNA polymerase to identify the virus. Preliminary DNA sequence analysis revealed the virus was most similar to rhesus macaque rhadinovirus (RRV). The complete sequence of the viral genome was determined and compared to simian and human herpesvirus genomes representing alpha-herpesviruses, beta-herpesviruses and gamma-1 and -2 herpesviruses. By this analysis, the JM herpesvirus, referred to as JM rhadinovirus (JMRV) is a gamma-2 herpesvirus most closely related to RRV, with 89.5% nucleotide sequence identity and secondarily related to human Kaposi sarcoma herpesvirus (KSHV) with 47.9% nucleotide sequence identity (Table 2). JMRV has subsequently been isolated from active CNS lesions of five other JM with JME, but has not been isolated from normal white matter from JM with or without JME.

DISCUSSION

JME appeared spontaneously in JM at the ONPRC 21 years after the colony was established. The initial case of JME occurred in 1986 and since then the disease typically has affected 1–3% of the colony each year, with two exceptions. JME usually occurs in young adult animals, but the disease can present in juvenile or aged animals, and shows no preference for either gender. Clinically, JME causes paralysis, ataxia and ocular motor paresis. While most animals failed to recover sufficiently to be safely returned to the colony, three monkeys recovered, were returned to the colony and then relapsed one or more years later. MRI of eight animals revealed changes similar to acute MS. Pathologically, JME causes multifocal areas of demyelination of varying acuity with loss of oligodendrocytes and variable axonal loss in the white matter of the cerebrum, cerebellum, brainstem and spinal cord associated with macrophages and lymphocytic infiltrates. Chronic inactive demyelinated lesions also occur, suggesting that asymptomatic lesions may occur before clinical JME. JME is the first naturally occurring inflammatory demyelinating disease in an NHP.

JME has clinical, MRI and pathologic similarities to MS. These include similar clinical manifestations, a relapsing course in monkeys that recovered sufficiently to be returned to the colony, MRI abnormalities like those of acute MS lesions and similar neuropathologic abnormalities, including plaque-like demyelinating lesions associated with lymphocytes and macrophages, oligodendrocyte depletion, limited remyelination and variable axonal loss. However, there are some features of JME that differ from MS. These include CSF containing neutrophils as well as lymphocytes in most cases and necrosis and hemorrhage as part of the pathologic continuum. These differences may represent species-specific differences in inflammatory and tissue responses. It is worth noting that EAE in NHP often has neutrophils in the CSF and necrosis and hemorrhage as part of the neuropathology, which differs from EAE in rodents[18]. Overall the clinical, MRI and neuropathologic features of JME have more similarities than differences with MS and JME is clearly an inflammatory demyelinating disease. Further investigations are needed to determine the full extent of similarities of JME with MS.

There are several features of JME that makes this an extremely appealing model for MS. First, the disease occurs spontaneously, which makes it distinct from current models of MS that require artificial manipulation to induce disease. Second, it affects a small percentage of animals in the colony, approximately 1–3% each year, suggesting there may be a genetic susceptibility to the disease as there is in MS. The ONPRC began tracing the pedigrees of the JM troop in 2000 utilizing specific microsatellite markers. Interestingly, animals developing JME since 2000 come from distinct matrilines from the original troop, supporting the idea that host genetic factors play a significant part in susceptibility to disease

(unpublished data). Determining the genetic factors that coincide with disease and predispose animals to develop JME is currently being explored on archived tissue and new cases. Third, like MS, JME is an inflammatory disease, suggesting either an autoimmune disease or a viral infection. An autoimmune pathogenesis of MS is commonly proposed but definitive evidence of this remains lacking. Auto-reactive T cells and anti-myelin antibodies have been proposed as being critical to the immunopathogenesis of MS[19–21]. We are currently assessing new cases of JME for anti-myelin T cell responses and antibodies against myelin antigens.

Finally, based on epidemiologically studies and the histopathology, a viral etiology for MS has long been suspected. Multiple candidate viruses have been proposed but none has been convincingly associated with the disease. Here, we report the isolation of a previously unknown herpesvirus, JMRV, isolated from acute JME lesions. We have been unable to isolate JMRV from normal appearing white matter of JM with and without JME. Complete DNA sequencing reveals this to be a rhadinovirus with significant sequence homologies with RRV and human KSHV. Reagents are being generated against this virus to evaluate the potential role of JMRV in JME. This is of particular interest since human Epstein-Barr virus and human herpesvirus 6 are two herpesviruses that have been implicated as playing a role in the pathogenesis of MS[22–30]. Demonstrating that a simian rhadinovirus induces JME will provide a new class of herpesvirus that would warrant investigation in MS.

In summary, JME is a unique spontaneous demyelinating disease in an NHP. Preliminary results suggest that the disease occurs in genetically predisposed monkeys and is associated with a novel simian herpesvirus. Further investigation of the pathogenesis of JME may provide new insights into the pathogenesis of MS.

Acknowledgments

The authors thank Ms. Lori Boshears and Mr. Andrew Townsend for assistance with the manuscript and figures, and members of the Division of Animal Resources for their diligence and care of the animals. This work was supported by the National Institutes of Health (NIH) Grant P51RR00163, the Research Enrichment Award Program of the Department of Veterans Affairs Biomedical Laboratory Research and Development, the OHSU Multiple Sclerosis Center, the United States Department of Defense (W81XWH-09-1-0276), OHSU/Vertex SRA-05-07-01 and NIH Grant R01-EB007258.

References

1. Noseworthy JH, Lucchinetti C, Rodriguez M, Weinshenker BG. Multiple sclerosis. N Engl J Med. 2000 Sep 28; 343(13):938–952. [PubMed: 11006371]
2. Libbey, J.; Fujinami, R. Potential Triggers of MS. In: Martin, R.; Lutterotti, A., editors. Molecular Basis of Multiple Sclerosis. Springer Berlin / Heidelberg: 2010. p. 21-42.
3. Libbey JE, Fujinami RS. Experimental autoimmune encephalomyelitis as a testing paradigm for adjuvants and vaccines. Vaccine. 2010 Sep 16. (epub).
4. Ferraro A, Cazzullo CL. Chronic experimental allergic encephalomyelitis in monkeys. J Neuropathol Exp Neurol. 1948 Jul; 7(3):235–260. [PubMed: 18872389]
5. Genain CP, Hauser SL. Creation of a model for multiple sclerosis in Callithrix jacchus marmosets. J Mol Med. 1997 Mar; 75(3):187–197. [PubMed: 9106075]
6. Rivers TM, Schwentker FF. Encephalomyelitis Accompanied by Myelin Destruction Experimentally Produced in Monkeys. J Exp Med. 1935 Apr 30; 61(5):689–702. [PubMed: 19870385]
7. t Hart BA, Massacesi L. Clinical, pathological, and immunologic aspects of the multiple sclerosis model in common marmosets (Callithrix jacchus). J Neuropathol Exp Neurol. 2009 Apr; 68(4):341–355. [PubMed: 19337065]
8. Miller SD, Vanderlugt CL, Begolka WS, et al. Persistent infection with Theiler's virus leads to CNS autoimmunity via epitope spreading. Nat Med. 1997 Oct; 3(10):1133–1136. [PubMed: 9334726]

9. Tsunoda I, Fujinami RS. Two models for multiple sclerosis: experimental allergic encephalomyelitis and Theiler's murine encephalomyelitis virus. J Neuropathol Exp Neurol. 1996 Jun; 55(6):673–686. [PubMed: 8642393]
10. Dal Canto MC, Lipton HL. Multiple sclerosis. Animal model:Theiler's virus infection in mice. Am J Pathol. 1977 Aug; 88(2):497–500. [PubMed: 195474]
11. Clatch RJ, Melvold RW, Dal Canto MC, Miller SD, Lipton HL. The Theiler's murine encephalomyelitis virus (TMEV) model for multiple sclerosis shows a strong influence of the murine equivalents of HLA-A, B, and C. J Neuroimmunol. 1987 Jun; 15(2):121–135. [PubMed: 3584435]
12. Wong SW, Bergquam EP, Swanson RM, et al. Induction of B cell hyperplasia in simian immunodeficiency virus-infected rhesus macaques with the simian homologue of Kaposi's sarcoma-associated herpesvirus. The Journal of experimental medicine. 1999 Sep 20; 190(6):827–840. [PubMed: 10499921]
13. Kornek B, Storch MK, Weissert R, et al. Multiple sclerosis and chronic autoimmune encephalomyelitis: a comparative quantitative study of axonal injury in active, inactive, and remyelinated lesions. Am J Pathol. 2000 Jul; 157(1):267–276. [PubMed: 10880396]
14. Prineas, JW. The neuropathology of multiples sclerosis. Koetsier, KC., editor. Amsterdam: Elsevier; 1985.
15. Raine, CS. Demyelinating diseases. 2nd ed. Davis RLaR, DM., editor. Baltimore, MD: 1990.
16. Lucchinetti CF, Bruck W, Rodriguez M, Lassmann H. Distinct patterns of multiple sclerosis pathology indicates heterogeneity on pathogenesis. Brain Pathol. 1996 Jul; 6(3):259–274. [PubMed: 8864283]
17. Ozawa K, Suchanek G, Breitschopf H, et al. Patterns of oligodendroglia pathology in multiple sclerosis. Brain. 1994 Dec; 117(Pt 6):1311–1322. [PubMed: 7820568]
18. Shaw, CM.; Alvord, EC, Jr. Treatment of experimental allergic encephalomyelitis in monkeys. II. Histopathological studies. In: Shiraki H, YT.; Kuroiwa, Y., editors. The Aetiology and Pathogenesis of the Demyelinating Diseases. Tokyo: Japan Science Press; 1976. p. 277-295.
19. Genain CP, Cannella B, Hauser SL, Raine CS. Identification of autoantibodies associated with myelin damage in multiple sclerosis. Nat Med. 1999 Feb; 5(2):170–175. [PubMed: 9930864]
20. Diaz-Villoslada P, Shih A, Shao L, Genain CP, Hauser SL. Autoreactivity to myelin antigens: myelin/oligodendrocyte glycoprotein is a prevalent autoantigen. J Neuroimmunol. 1999 Sep 1; 99(1):36–43. [PubMed: 10496175]
21. Koehler NK, Genain CP, Giesser B, Hauser SL. The human T cell response to myelin oligodendrocyte glycoprotein: a multiple sclerosis family-based study. J Immunol. 2002 Jun 1; 168(11):5920–5927. [PubMed: 12023398]
22. Alvarez-Lafuente R, Martin-Estefania C, de Las Heras V, et al. Active human herpesvirus 6 infection in patients with multiple sclerosis. Arch Neurol. 2002 Jun; 59(6):929–933. [PubMed: 12056928]
23. Ascherio A. Epstein-Barr virus in the development of multiple sclerosis. Expert Rev Neurother. 2008 Mar; Mar(3):331–333. [PubMed: 18345964]
24. Ascherio A, Munch M. Epstein-Barr virus and multiple sclerosis. Epidemiology. 2000 Mar; 11(2): 220–224. [PubMed: 11021623]
25. Ascherio A, Munger KL, Lennette ET, et al. Epstein-Barr virus antibodies and risk of multiple sclerosis: a prospective study. JAMA. 2001 Dec 26; 286(24):3083–3088. [PubMed: 11754673]
26. Carrigan DR, Harrington D, Knox KK. Subacute leukoencephalitis caused by CNS infection with human herpesvirus-6 manifesting as acute multiple sclerosis. Neurology. 1996 Jul; 47(1):145–148. [PubMed: 8710068]
27. Carrigan DR, Knox KK. Human herpesvirus six and multiple sclerosis. Mult Scler. 1997 Dec; 3(6): 390–394. [PubMed: 9493640]
28. Cepok S, Zhou D, Srivastava R, et al. Identification of Epstein-Barr virus proteins as putative targets of the immune response in multiple sclerosis. J Clin Invest. 2005 May; 115(5):1352–1360. [PubMed: 15841210]

29. Challoner PB, Smith KT, Parker JD, et al. Plaque-associated expression of human herpesvirus 6 in multiple sclerosis. Proc Natl Acad Sci U S A. 1995 Aug 1; 92(16):7440–7444. [PubMed: 7638210]

30. Christensen T. The role of EBV in MS pathogenesis. Int MS J. 2006 May; 13(2):52–57. [PubMed: 16635422]

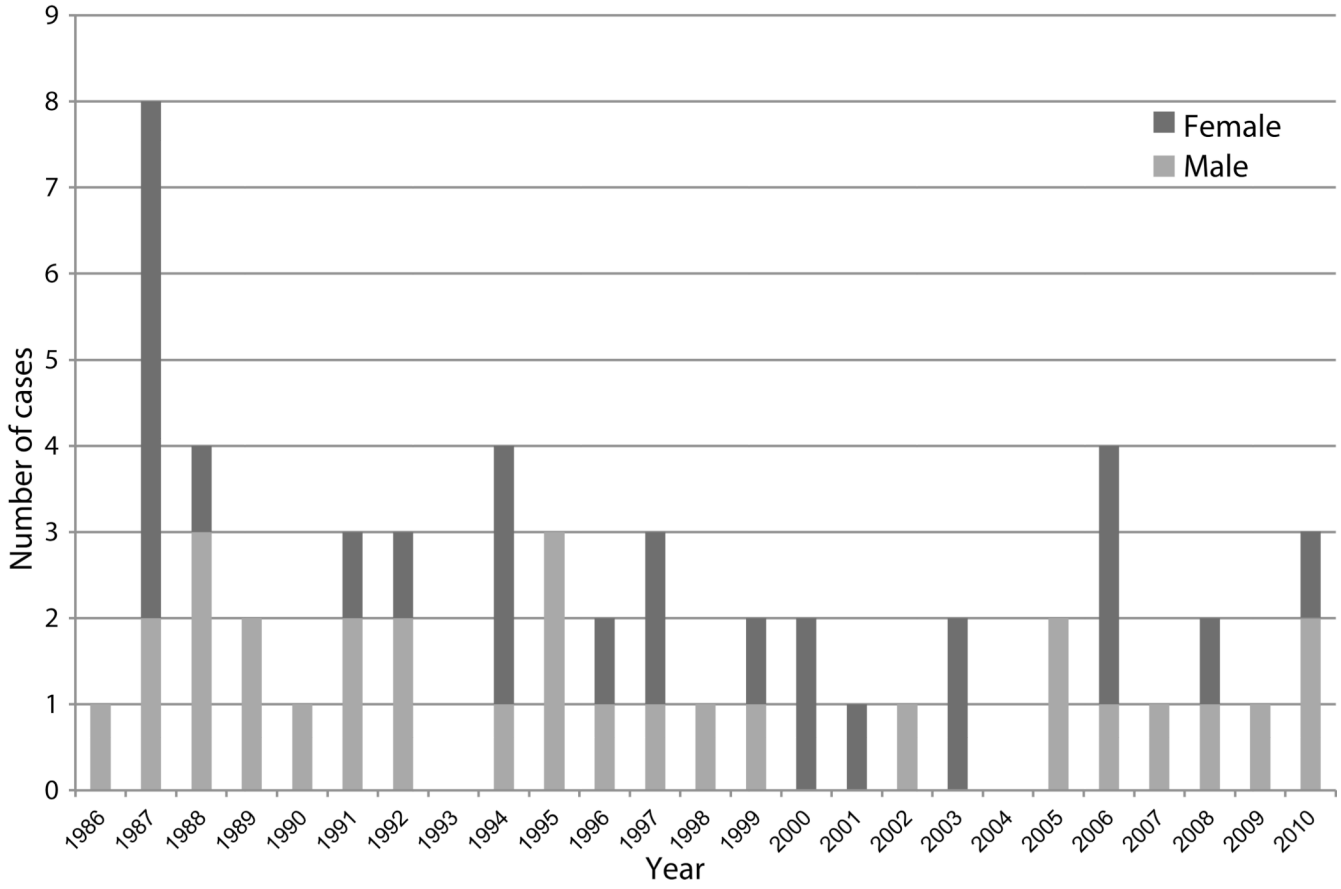

Figure 1.
Number of Japanese macaques affected each year with Japanese macaque encephalomyelitis (JME).

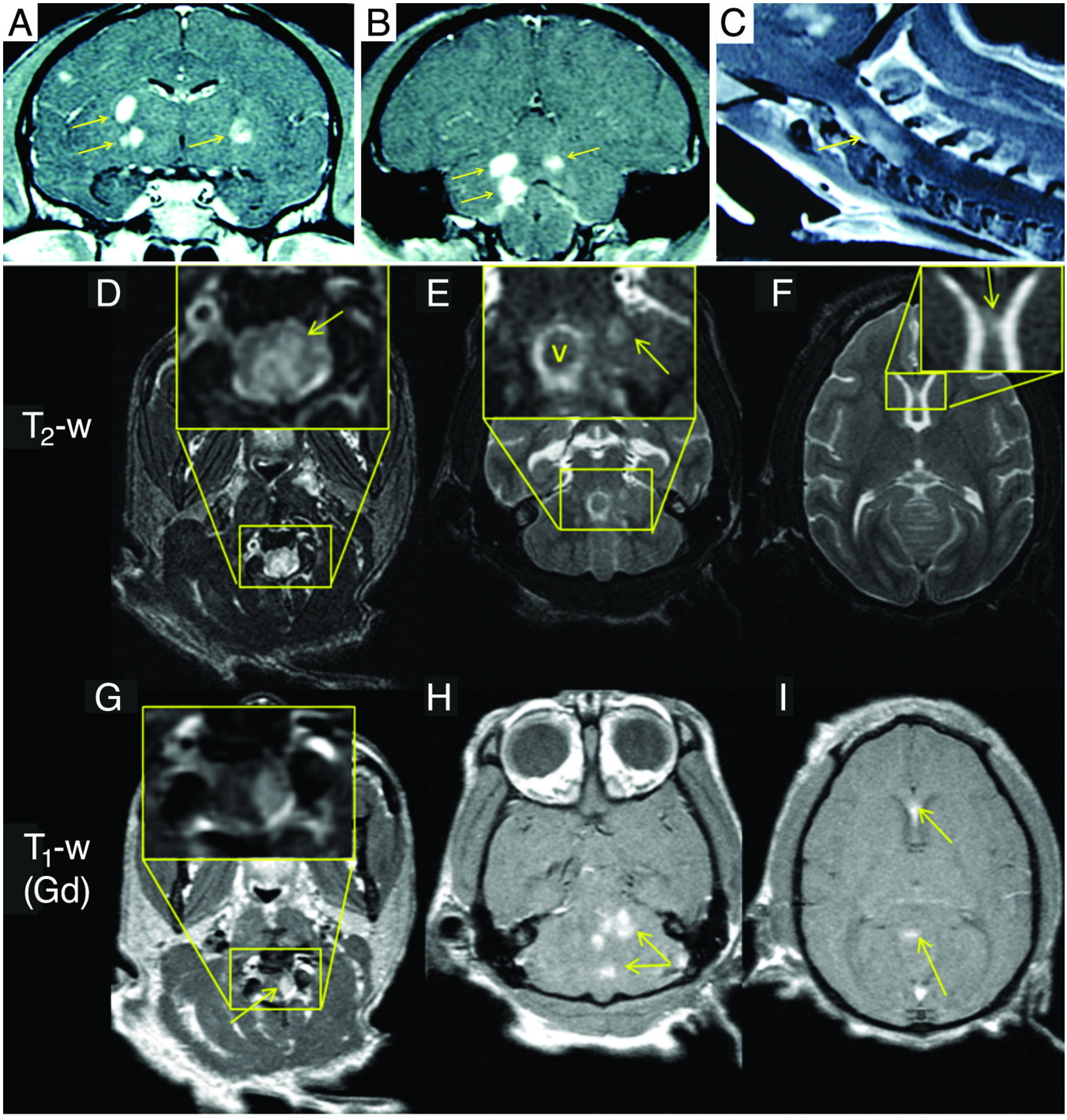

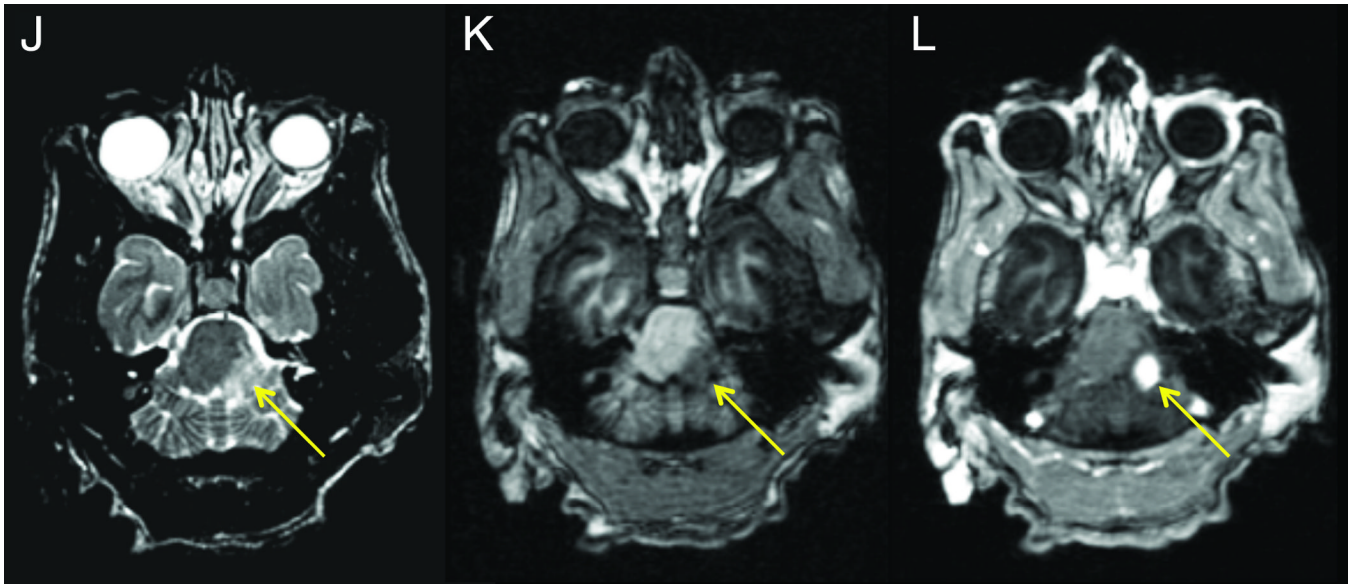

Figure 2. MRI of animals with JME

Panels A–C, post-gadolinium T_1-weighted MRI images from JM #19384 11 days after presentation with acute flaccid paralysis of the right pelvic limb. (A) Coronal image of cerebral hemispheres reveals gadolinium-enhanced lesions (arrows) in the internal capsule. (B) Coronal image of posterior cerebral hemispheres, cerebellum and brainstem shows 3 gadolinium-enhanced lesions in corpus medullare (arrows) of the cerebellum. (C) Sagittal image of upper cervical cord shows gadolinium-enhanced lesion (arrow). Panels D–I, axial 3Y MRI images from JM #26174 obtained 4 days after developing signs of JME. (D) Axial T_2-weighed image of upper cervical spinal cord shows hyperintense signal that is expanded in insert and identified (arrow). (E) Hyperintense signal in cerebellar region that is expanded in insert and denoted (arrow). The hyperintense ring surrounding “v” in the insert is CSF fluid superior to the 4^{th} ventricle adjacent to the superior medullary velum. (F) Hyperintense signal in the genu of the corpus callosum that is expanded in the insert and identified (arrow). Axial post-gadolinium T_1-weighted image shows enhancing lesions in upper cervical spinal cord (G), cerebellum (H), and genu of the corpus callosum (I). Panels J–L, axial 3T MRI images from JM #13221 during the acute phase of JME. (J) Axial T_2-weighted image shows hyperintense lesion in the left lateral pons and peduncule (arrow) that is hypointense on a T_1-weighted pre-contrast MPRAGE (K, arrow) image. The lesion enhances on a T_1-weighted MPRAGE image acquired 30 min after the administration of 0.2 mmol/kg gadoteridol (L, arrow.)

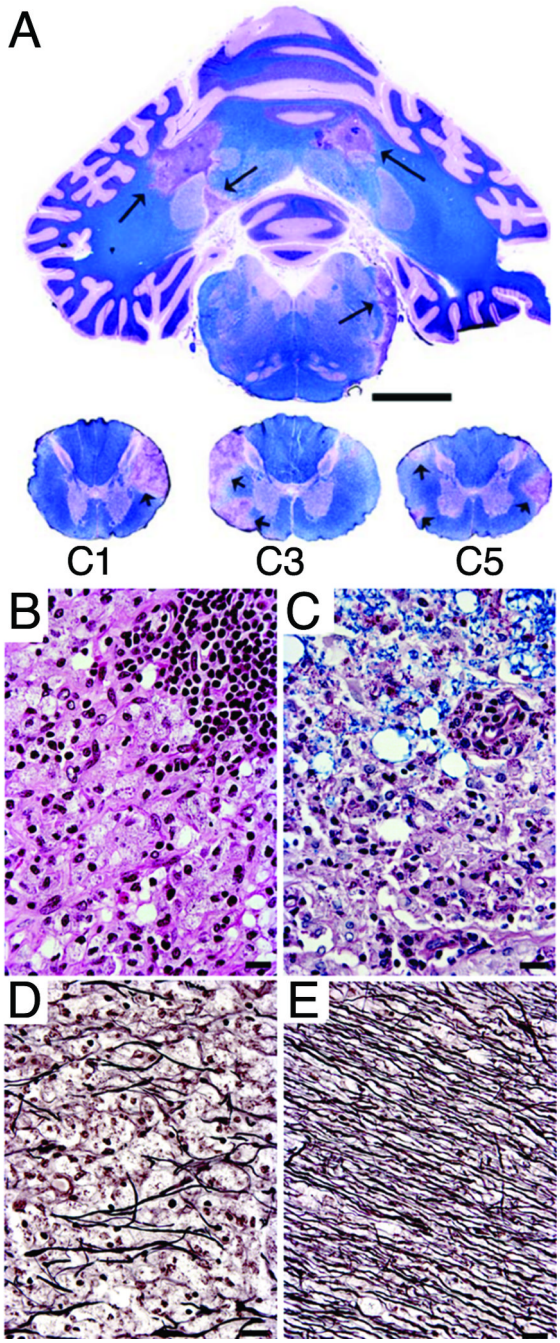

Figure 3. Histopathology of JME

Histopathological examination of the brain of JM #19384 obtained 53 days following clinical presentation of JME. (A) Luxol fast blue-PAS-hematoxylin stain of cerebellum and cervical spinal cord. Note the large, well-defined, irregular-shaped areas of myelin loss in the corpus medullare of the cerebellum (arrows) corresponding to the lesions seen 42 days earlier in the MRI images (Figure 2B). Similar lesions are present in the lateral white matter columns of the 1st, 2nd and 5th cervical spinal cord segments (arrows); the abnormalities in the upper cervical cord correspond to lesions seen on MRI (Figure 2C); scale bar, 1 cm. (B) High power magnification of a portion of the large chronic active plaque in the upper left of the cerebellum. Normal appearance of white matter is obliterated by large foamy

macrophages and scattered lymphocytes. Swollen myelin sheaths appear as circular optically clear spaces. A portion of a thick perivascular lymphocytic cuff is present in the upper right of the panel. Hematoxylin-eosin stain; scale bar, 50 μm. (C) Portion of a chronic inactive plaque from the cerebellum. Note that the myelin in the upper portion of the panel is vesiculated but retains Luxol fast blue staining. Macrophages containing reddish PAS-stained debris and astrocytes obliterate normal white matter architecture in the bottom portion of the panel. Luxol fast blue-PAS-hematoxylin stain; scale bar, 50 μm. (D and E) Reduced number of axons in the center of a chronic inactive plaque (D) compared to normal axonal density in normal appearing white matter (E). Bielschowsky's silver impregnation axonal stain; scale bar, 50 μm.

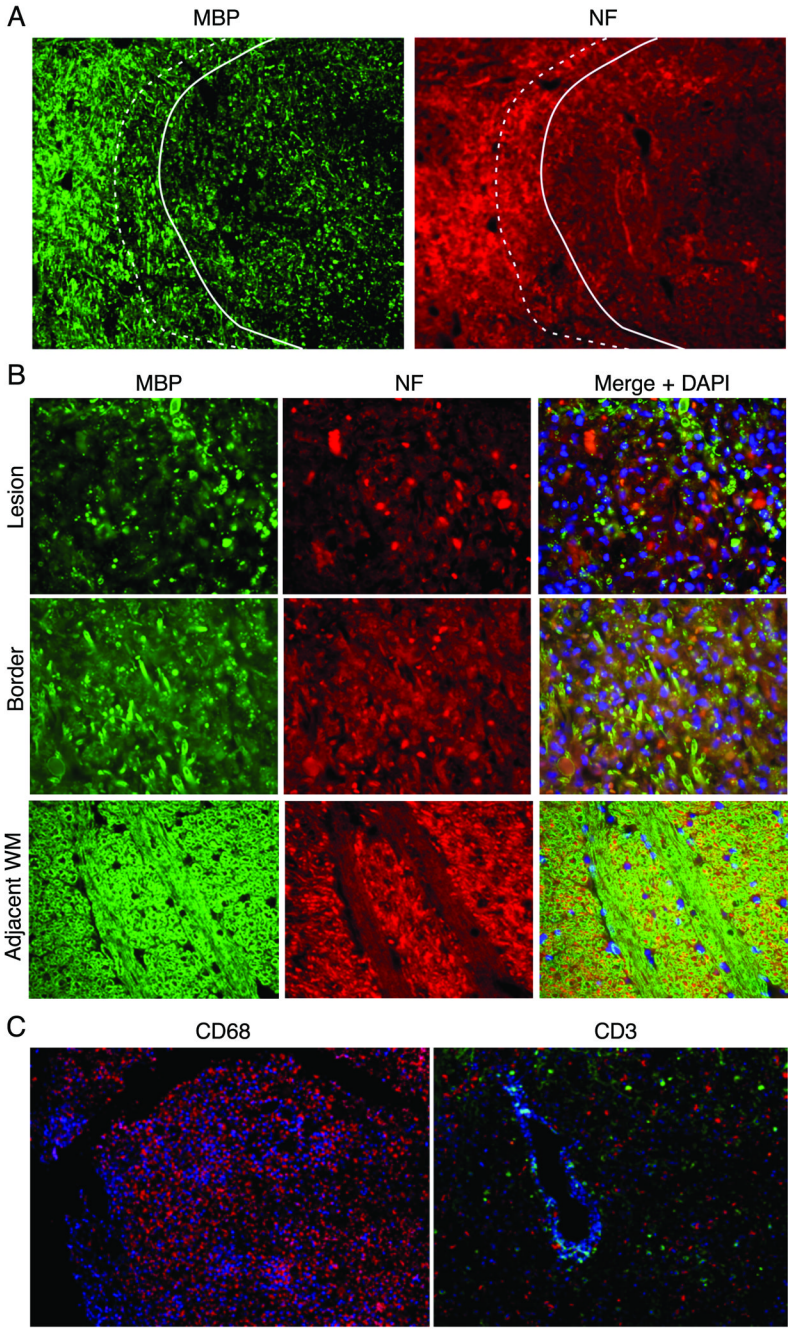

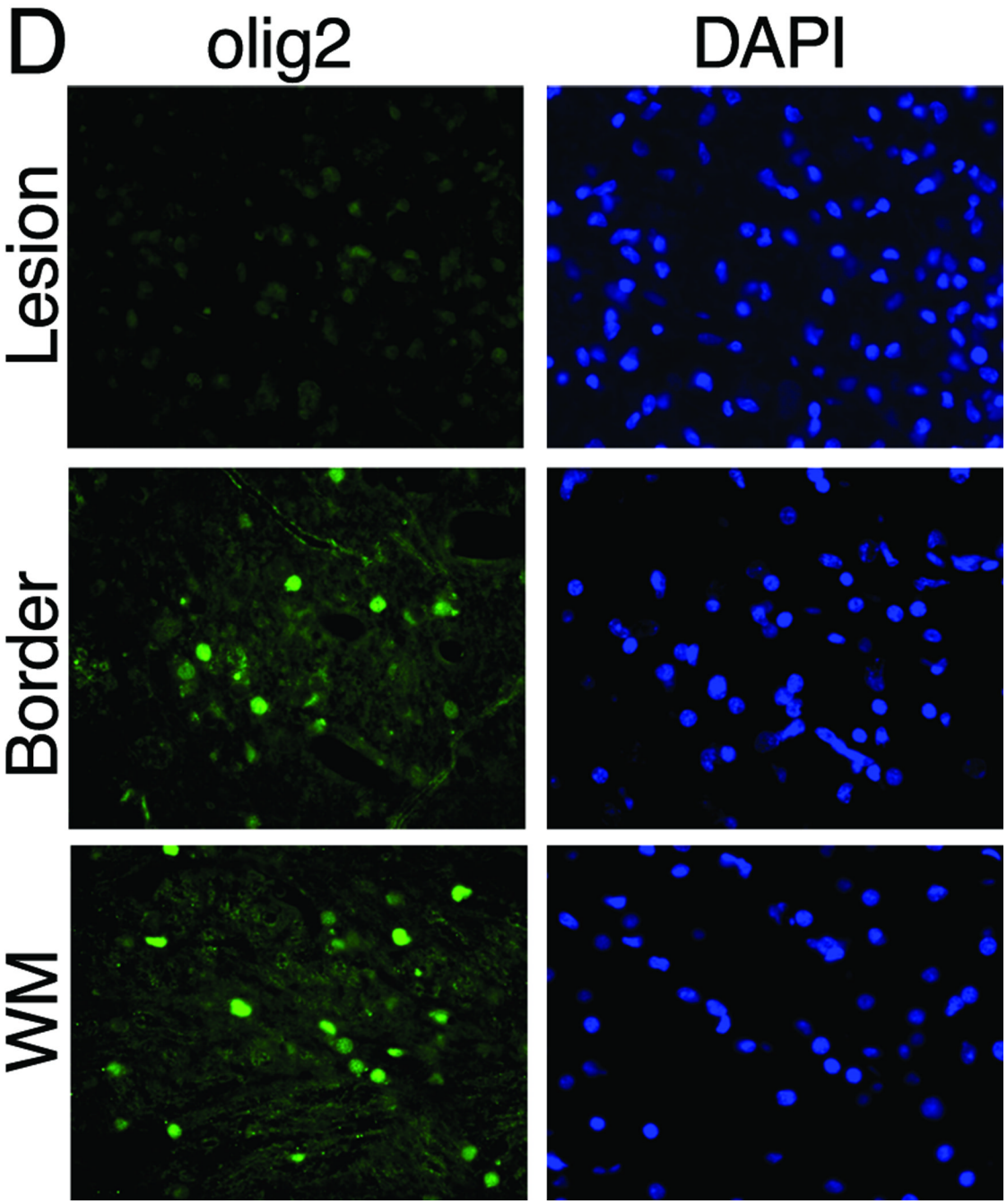

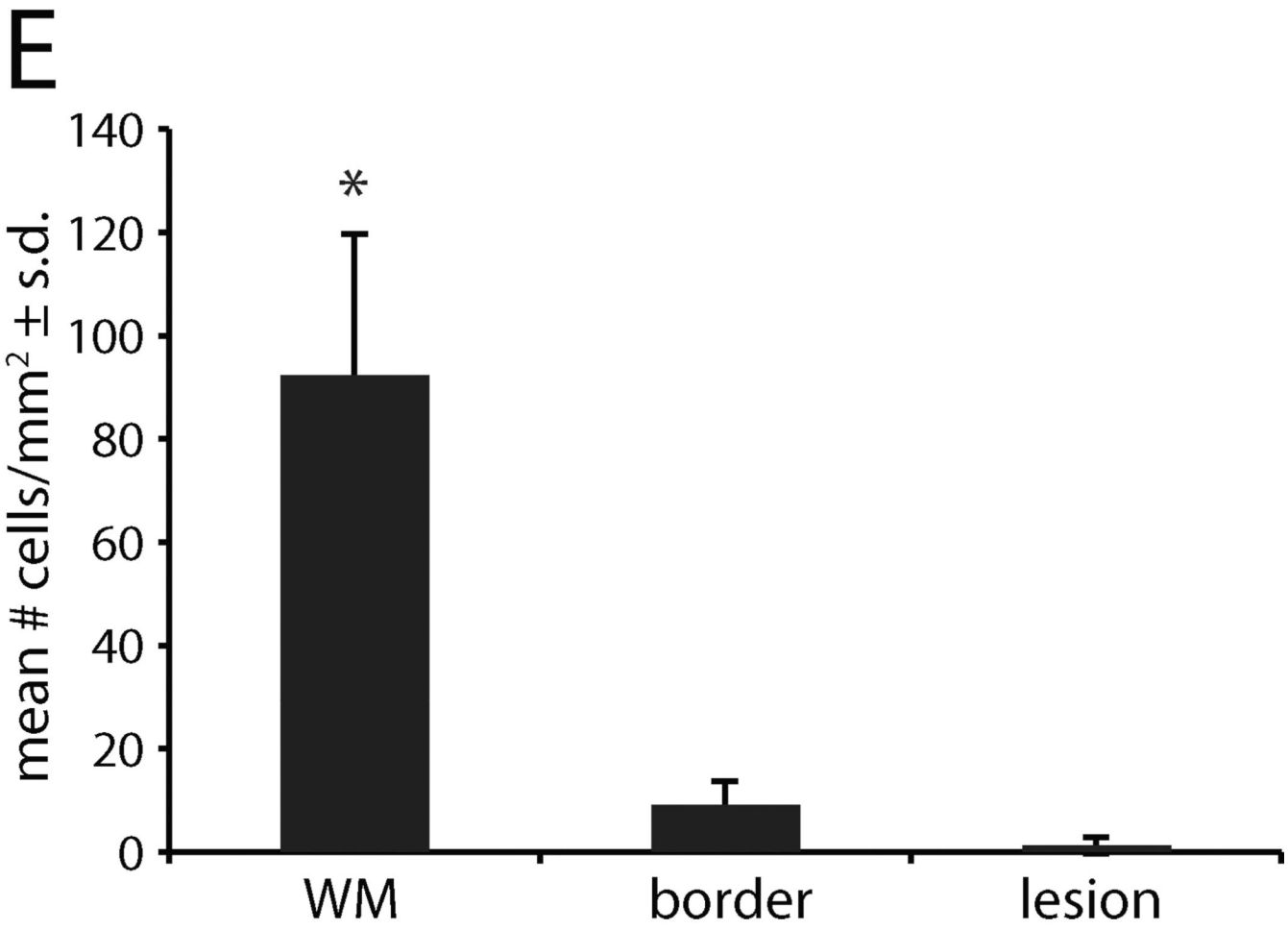

Figure 4. Demyelination and axonal loss in JME lesion

Immunofluorescent imaging from pontine lesion from JM #13221 identified by MRI (Figure 2J–L) .(A) The pontine lesion was double labeled for MBP (green) and NF (red) to visualize demyelination and loss of neurons. Area to the right of the solid line demarcates demyelinated lesion and shows marked reduction in staining for MBP and NF, indicating loss of myelin and axons; dashed line is lesion border with mix of damaged myelin and normal appearing myelin. Area to the left of the dashed line is unaffected white matter (WM) (5× magnification). (B) High magnification images of the lesion, border and unaffected white matter stained for the presence of MBP, NF and DAPI for nuclei to visualize the extent of demyelination and axonal damage. Note reduction in MBP and NF staining in both the lesion and border areas. The merged image of lesion and border reveals increased cellularity (increased DAPI staining), some preserved myelinated axons and some NF+ axons without myelin. (40× magnification). (C) A cerebellar lesion from JM #13221 showing CD68+ macrophages (red) and CD3+ T cells (green) near a venule (blue) (10× and 20× magnification, respectively). (D) The lesion site in (A) was immunostained for olig2 to assess the presence of oligodendrocytes and with a nuclear stain (DAPI) in the lesion, border and unaffected white matter (WM). Note the reduction in staining in the sections from the lesion and border areas for olig2 with increased numbers of DAPI+ cells (40× magnification). (E) Quantification of olig2 immuno-labeling. Three adjacent sections were analyzed and three random fields in each section were counted at the lesion, lesion border,

and in adjacent white matter, showing significant reduction in olig2+ cells in the lesion and border compared with normal white matter ($p<0.01$).

Ann Neurol. Author manuscript; available in PMC 2012 September 1.

Table 1

Clinical Findings in Cases of JME

ID#	Sex	Age at Onset (Years/Day)	Duration of Disease prior to Euthanasia (Days)	Paresis	Ataxia	Optical	Other	CSF Cells/ mm^3 (% lymphocyte/ neutrophil)	CSF Protein mg/dL
13762	M	1Y76D	6	X				1 (ND)	20
03246	F	20Y17D	61				X		
14871	F	0Y94D	3		X			336 (ND)	0
12800	X**	4Y95D	14	X	X	X		186 (ND)	107
14528	X	1Y46D	52		X	X			
14873	M	0Y164D	4			X			
13754	M	2Y104D	2				X	2,710 (ND)	112
07804	F	12Y116D	14		X	X		58 (ND)	0
09179	F	10Y136D	83	X				0 (ND)	11
08234	F	12Y112D	20	X		X		11 (ND)	104
14214	M	2Y64D	0				X		
15535	M	0Y123D	3				X		
13998	M	3Y122D	13		X				
08420	M	13Y19D	4		X			30 (ND)	113
13752	M	3Y336D	3		X				
12113	M	7Y325D	22		X			0 (ND)	22
13768	F	6Y259D	2	X		X		112 (ND)	50
15997	M	1Y336D	1	X				83 (ND)	71
16376	M	0Y327D	2		X			204 (ND)	29
16387	M	1Y235D	7	X				70 (ND)	48
13744	X	7Y185D	6		X			8 (ND)	12
13993	M	6Y337D	0				X		
15306	M	5Y272D	5	X	X	X		12 (ND)	195
12817	F	11Y31D	13	X				20 (ND)	29
11032	F	14Y133D	6				X	68 (ND)	16
12059	F	12Y251D	3		X			10 (ND)	70
17792	M	1Y258D	5	X				385 (ND)	86

ID#	Sex	Age at Onset (Years/Day)	Duration of Disease prior to Euthanasia (Days)	Paresis	Ataxia	Optical	Other	CSF Cells/ mm^3 (% lymphocyte/ neutrophil)	CSF Protein mg/dL
16777	M	3Y354D	20		X	X		2 (ND)	10
12068*	M	13Y86D	4	X				174 (ND)	16
18247	M	1Y245D	16	X		X		87 (ND)	39
18925	F	0Y197D	7	X				22 (ND)	21
19325	M	0Y250D	2	X					
19085	F	1Y111D	49	X				58 (ND)	17
19395	F	0Y305D	1		X	X			
16746	F	7Y125D	5	X				20 (ND)	37
19894	M	1Y220D	0	X					
20472	F	0Y291D	0	X				108 (ND)	50
19400	F	3Y210D	19	X				541 (ND)	144
19384	F	4Y188D	53	X				88 (10/90)	103
16749+	F	9Y259D	124		X			56 (75/25)	21
12812	M	18Y207D	10	X				60 (86/14)	104
22699	F	1Y212D	6	X				230 (26/74)	55
22007	F	2Y351D	13	X				353 (92/8)	63
24059	M	1Y303D	3	X				408 (68/32)	0
24043	M	2Y180D	1	X					
24631	F	1Y225D	5	X					
22720	F	4Y203D	13	X				3 (100)	6
21282	F	6Y359D	32	X				9 (20/80)	7
18270	M	12Y38D	6	X				70 (25/75)	15
21255++	M	8Y93D	0	X					
26174	M	2Y225D	4	X				650 (25/75)	168
27616	F	0Y217D	1	X				123 (61/39)	55
18276	M	14Y321D	6		X				
20482	M	11Y304D	13		X			37 (71/29)	14
28422	M	0Y276D	6				X	11 (80/20)	25
13221	X**	26Y49D	1		X				

The clinical presentation of JMs with JME is similar to MS. Ataxia, paralysis or paresis of one or more limbs, and ocular abnormalities clinically characterizes JME.

* Animal 12068 had an initial episode of JME at 5 years 281 days and a second episode at 13 years 90 days.

+ Animal 16749 had an initial episode at 9 years 212 days and a second episode at 10 years 18 days.

++ Animal 21255 had an initial episode at 341 days and a second episode at 8 years 93 days.

** X refers to a female pseudohermaphroditic animal.

ND = no data.

Table 2

Clustal W alignment of JMRV genome with select simian and human herpesvirus genomes showing percent nucleotide sequence identity

Virus	JMRV	RRV	KSHV	HVS	RhLCV	EBV	RhCMV	HHV-6A	HHV-6B	HB virus	SVV	HSV-1
JMRV	100	89.5	47.9	35.0	27.9	22.3	19.5	27.2	26.2	27.1	31.3	25.6
RRV	89.5	100	48.3	34.7	28.3	22.6	19.9	27.6	26.5	27.6	31.5	26.1
KSHV	47.9	48.3	100	32.3	27.3	22.2	19.5	26.7	25.7	27.3	29.3	26.1
HVS	35.0	34.7	32.3	100	20.2	19.4	15.9	23.5	22.8	18.6	30.7	19.4
RhLCV	27.9	28.3	27.3	20.2	100	53.1	23.2	26.1	25.1	28.3	21.7	25.8
EBV	22.3	22.6	22.2	19.4	53.1	100	23.1	22.0	21.3	23.2	20.5	22.7
RhCMV	19.5	19.9	19.5	15.9	23.2	23.1	100	22.3	22.6	20.0	17.0	18.9
HHV-6A	27.2	27.6	26.7	23.5	26.1	22.0	22.3	100	88.3	25.2	24.6	24.0
HHV-6B	26.2	26.5	25.7	22.8	25.1	21.3	22.6	88.3	100	25.0	23.7	23.7
HB virus	27.1	27.6	27.3	18.6	28.3	23.2	20.0	25.2	25.0	100	21.4	49.5
SVV	31.3	31.5	29.3	30.7	21.7	20.5	17.0	24.6	23.7	21.4	100	21.9
HSV-1	25.6	26.1	26.1	19.4	25.8	22.7	18.9	24.0	23.7	49.5	21.9	100

JMRV, Japanese macaque rhadinovirus (GenBank accession number AY528864.1); RRV, rhesus macaque rhadinovirus (GenBank accession number AF083501); KSHV, Kaposi sarcoma-associated herpesvirus (GenBank accession number U75698); HVS, Herpesvirus saimiri (GenBank accession number NC_001350); RhLCV, rhesus lymphocryptovirus (GenBank accession number AY037858); EBV, Epstein Barr virus (GenBank accession number V01555); RhCMV, rhesus cytomegalovirus (GenBank accession number NC_006150); HHV-6A, human herpesvirus 6A (GenBank accession number NC_001664); HHV-6B, human herpesvirus 6B (GenBank accession number AF157706); HB virus, herpes B virus (GenBank accession number NC_004812); SVV, simian varicella virus (GenBank accession number NC_002686); HSV-1, herpes simplex virus type 1 strain F (GenBank accession number GU734771)